Temperature-Dependent Study on L-band EDFA Characteristics Pumped at 980nm and 1480nm in Phosphorus and Aluminum-rich Erbium-Doped Silica Fibers

Ziwei Zhai, Arindam Halder, Martín Núñez-Velázquez, and Jayanta K. Sahu

***Abstract*—In this paper, we present a comparative study on temperature-dependent spectroscopic characteristics and L-band amplifier performance for aluminum-rich erbium-doped fiber (EDF) and in-house fabricated phosphorus co-doped EDF. Different pumping configurations were studied to conclude that the pump wavelength of 980nm with unequal forward/backward pump powers exhibited better temperature stability. Phosphorus EDF provided 19.4±1.4dB gain and 4.6±0.2dB noise figure (NF) from 1575-1615nm at room temperature (RT), for a multi-channel input signal of -25dBm in each channel, whereas the aluminum-rich EDF provided 20.3±5.1dB gain and 5.3±0.8dB NF. Using a single-channel input signal of -25dBm at 1625nm, phosphorus EDF maintained >10dB gain with a 9.6dB and 12dB gain increment than aluminum-rich EDF at RT and -60ºC, respectively. The temperature-dependent gain (TDG) coefficient from 1575-1615nm was in the range -0.006 to -0.044 dB/ºC for phosphorus EDF and 0.011 to -0.023 dB/ºC for aluminum-rich EDF, over the temperature range -60 to +80ºC. We propose a hybrid L-band amplifier concatenating aluminum-rich EDF with phosphorus EDF, to suppress the temperature dependence of phosphorus EDF and improve the gain bandwidth restriction of aluminum-rich EDF. The hybrid EDF exhibited multi-channel 20.9±3.9dB gain and 3.7±0.6dB NF from 1575-1615nm at RT. The TDG coefficient of the hybrid EDF remained almost constant from 1585-1615nm, contributing to a temperature-insensitive gain flatness.**

***Index Terms*—Erbium-doped fiber (EDF); L-band optical amplifier; Phosphosilicate fiber; Temperature-dependent gain (TDG).**

I. Introduction

THE huge consumption of currently available transmission capacity leads to the demand in studying wideband and flat-gain amplifiers that can overcome the bandwidth limitations in the L-band of conventional erbium-doped fiber amplifiers (EDFAs). One limitation on the further capacity improvement of EDFs is the undesired loss due to excited state absorption (ESA) at the longer wavelength side of the L-band. Techniques to overcome the bandwidth restrictions were investigated using novel co-dopants and glass compositions with an intrinsically broader gain spectrum, as a result of shifting the $^4I_{13/2}$-$^4I_{9/2}$ transition of signal ESA to longer wavelengths [1, 2]. With strong mechanical and thermal stabilities, and low-loss, silica host fibers are more beneficial with no splicing problem when fusion spliced to standard single-mode fiber (SMF). Phosphorus/aluminum (P/Al) co-doped silica EDFs have been employed to extend the erbium gain profile. Compared to Al co-doped silica EDFs, a higher P/Al ratio is more preferable to redshift the L-band gain [3, 4].

As a significant evaluation factor of environmental robustness, the good thermal stability of EDFA is desired. Temperature-dependent gain and noise figure (NF) performances for EDFAs are due to the thermal effect on the re-distribution of ions in the sublevels of the ground and metastable states according to Boltzmann's law, resulting in the temperature-dependent absorption and emission cross-sections [5]. It was reported that EDFAs are more temperature-sensitive when pumped at 1480nm than 980nm [6, 7] and more temperature-sensitive in the L-band than in the C-band [8, 9]. However, there are few reports on the temperature dependence of EDFAs covering the longer wavelength side of the L-band (up to 1625nm) and few comparative discussions on different pump wavelengths for the L-band EDFAs.

In this paper, we report the temperature-dependent spectroscopic characteristics and amplifier performance for our in-house fabricated phosphorus co-doped silica EDF (EDF1/P) and one conventional aluminum-rich L-band EDF (EDF2/Al). We studied different pumping configurations of equal and unequal forward/backward (FW/BW) pumps at two pump wavelengths of 980nm and 1480nm. We studied the multi-channel gain and NF from 1575 to 1615nm and single-channel gain and NF from 1575 to 1625nm, under the temperature range from -60 to 80ºC. To the best of our knowledge, our study has extended to a longer wavelength of 1625nm compared to

Manuscript received xx xx, xxxx; revised xx xx, xxxx; accepted xx xx, xxxx. Date of publication xx xx, xxxx; date of current version xx xx, xxxx.

The authors are with Optoelectronics Research Centre, University of South ampton, Southampton, SO17 1BJ, U.K. (e-mail: Z.Zhai@soton.ac.uk; A.Halder@soton.ac.uk; M.M.A.Nunez-Velazquez@soton.ac.uk; jks@orc.soton.ac.uk). *(Corresponding author: Ziwei Zhai.)*

Color versions of one or more of the figures in this article are available online at https://ieeexplore.ieee.org.

Digital Object Identifier XXXXXXXXXX.

previous temperature-dependent L-band EDFA studies [8, 10]. The unequal FW/BW pumps at 980nm provided a less temperature-dependent amplifier performance in the L-band. At 1615nm, EDF1/P provided a gain increment of 3.6dB and 5.9dB over EDF2/Al at room temperature (RT, 20ºC) and -60ºC, respectively. Gain increment at 1625nm was 9.6dB at RT and 12dB at -60ºC. EDF1/P was advantageous in extending the L-band gain bandwidth but exhibited a slightly higher temperature sensitivity. We propose a technique to balance the temperature sensitivity and longer wavelength limit in L-band gain by concatenating EDF2/Al and EDF1/P, with a flattened TDG coefficient and lower NF. From 1575 to 1615nm, the TDG coefficient of the hybrid EDF had a negligible variation of 0.007dB/ºC and 0.003dB/ºC when using unequal and equal pumps, respectively.

II. Spectroscopic Characteristics

The gain of EDFA can be expressed by (1), where Γ is the mode overlap factor, L is the device length, N_1 and N_2 are the populations of erbium ions on the lower and upper level of the stimulated emission transmission, respectively [11]. Temperature-dependent σ_a and σ_e are the absorption and emission cross-sections, respectively, which determine the TDG performance. In addition to the cross-sections, Boltzmann distribution law needs to take into consideration in the 1480nm pump condition [12]. The EDFA gain strongly depends on the population inversion level. The relative population difference (i.e., $\Delta N/N=(N_2-N_1)/N$) of 1480nm pump condition considers the Boltzmann factor β, described by (2)-(4) [13]. W_{sa}, W_{se} and R_p are the absorption and stimulated emission rates in the signal band, and the pump rate, respectively. τ is the lifetime, k_B is the Boltzmann constant, T is the temperature in Kelvin. N is the total number of erbium ions in the three-level system. N_3 is the erbium ion population on the pump level. ΔE_3 represents the energy difference between the pump level and upper level of the stimulated emission transmission. While the effect of β is negligible in the case of 980nm pump condition, as the erbium population of pump level $^4I_{11/2}$ is negligible, i.e., $N_3=0$ [14]. As a result, the 1480nm pump condition has a more temperature-dependent amplifier performance compared with the 980nm pump condition.

$$G(\lambda)=\exp\left\{\left[\sigma_e(\lambda)N_2-\sigma_a(\lambda)N_1\right]\Gamma L\right\} \tag{1}$$

$$\frac{\Delta N}{N}=\frac{R_p\tau(1-\beta)+W_{sa}\tau(1-\eta)-1}{R_p\tau(1+2\beta)+W_{sa}\tau(1+\eta+\beta)+1} \tag{2}$$

$$\beta=\frac{N_3}{N_2}=\exp\left(\frac{-\Delta E_3}{k_BT}\right) \tag{3}$$

$$\eta=\frac{W_{se}}{W_{sa}} \tag{4}$$

We fabricated the erbium-doped phosphosilicate preform using the solution doping method along with the modified chemical vapor deposition (MCVD) technique. Then, the preform was drawn into a fiber with a core/cladding diameter of 5.6/125μm, an LP_{11} cutoff wavelength of 1335nm, and a numerical aperture (NA) of 0.203. One commercial L-band EDF (OFS-LRL61373) with a core/cladding diameter of 3.5/125μm and NA of 0.258 had an LP_{11} cutoff wavelength of 1184nm. The basic characteristics measured at RT for the two EDFs are presented in Table 1. The absorption (Abs) and background loss (BL) were measured based on the cutback method. The unsaturable loss (UL), expressed in percentage, is the ratio of the unsaturable absorption coefficient to the small-signal absorption coefficient as increasing the launched pump power.

TABLE I
Basic Characteristics of EDFs in This Work

	EDF1/P	EDF2/Al
Abs@980nm (dB/m)	8.5	12.8
Abs@1480nm (dB/m)	8.8	15.1
Peak Abs (dB/m)	26 (@1534.5nm)	31 (@1528.8nm)
UL@980nm (%)	8.8	2.0
UL@1480nm (%)	2.3	2.3
BL@1200nm (dB/km)	17	7.3
LP_{11} mode cutoff (nm)	1335	1184
Core/cladding (um)	5.6/125	3.5/125
Numerical aperture	0.203	0.258

To study the temperature-dependent spectroscopic characteristics, the absorption, fluorescence, and lifetime of EDF1/P and EDF2/Al were measured over the temperature range -60 to 80ºC. Then, the temperature-dependent absorption and emission cross-sections (TDσ_a and TDσ_e) were calculated based on the Füchtbauer-Ladenburg (FL) equation and McCumber theory [15]. FL equation was used to derive the emission cross-sections from the measured fluorescence spectrum and lifetime, described by (5). McCumber theory relates the absorption and emission cross-sections, described by (6). n is the refractive index of the fiber core, c is the vacuum velocity of light, h is the Planck constant, ε is the net free energy. τ is the lifetime. $F(\lambda)$ is the fluorescence intensity. Fig. 1 (a) and (b) show σ_a and σ_e at -60ºC, RT, and 80ºC for EDF1/P and EDF2/Al. We defined the temperature-dependent cross-section (TDσ) coefficient as the slope of the linear regression fit between the cross-section and the corresponding temperature. TDσ_a and TDσ_e coefficients at the pump wavelength of 1480nm were -2.39×10^{-28}m^2/ºC and 2.39×10^{-28}m^2/ºC for EDF1/P, and -1.73×10^{-28}m^2/ºC and 2.40×10^{-28}m^2/ºC for EDF2/Al, as shown in the insets of Fig. 1 (a) and (b). TDσ_a coefficients at the pump wavelength of 980nm were -2.11×10^{-28}m^2/ºC and -1.22×10^{-28}m^2/ºC for EDF1/P and EDF2/Al, respectively. 980nm pump condition had zero-σ_e and less TDσ_a coefficient (absolute value), indicating a less temperature-sensitive amplifier performance compared to the pump wavelength of 1480nm. Similarly, with less TDσ_a coefficients (absolute value) at both 980nm and 1480nm, EDF2/Al was expected to be less temperature-sensitive than EDF1/P. Also, σ_e at the signal wavelengths were less temperature-dependent for EDF2/Al, as shown in Fig. 1 (c). The temperature-dependent lifetime of two

This article has been accepted for publication in a future issue of this journal, but has not been fully edited. Content may change prior to final publication. Citation information: DOI 10.1109/JLT.2022.3167261, Journal of Lightwave Technology

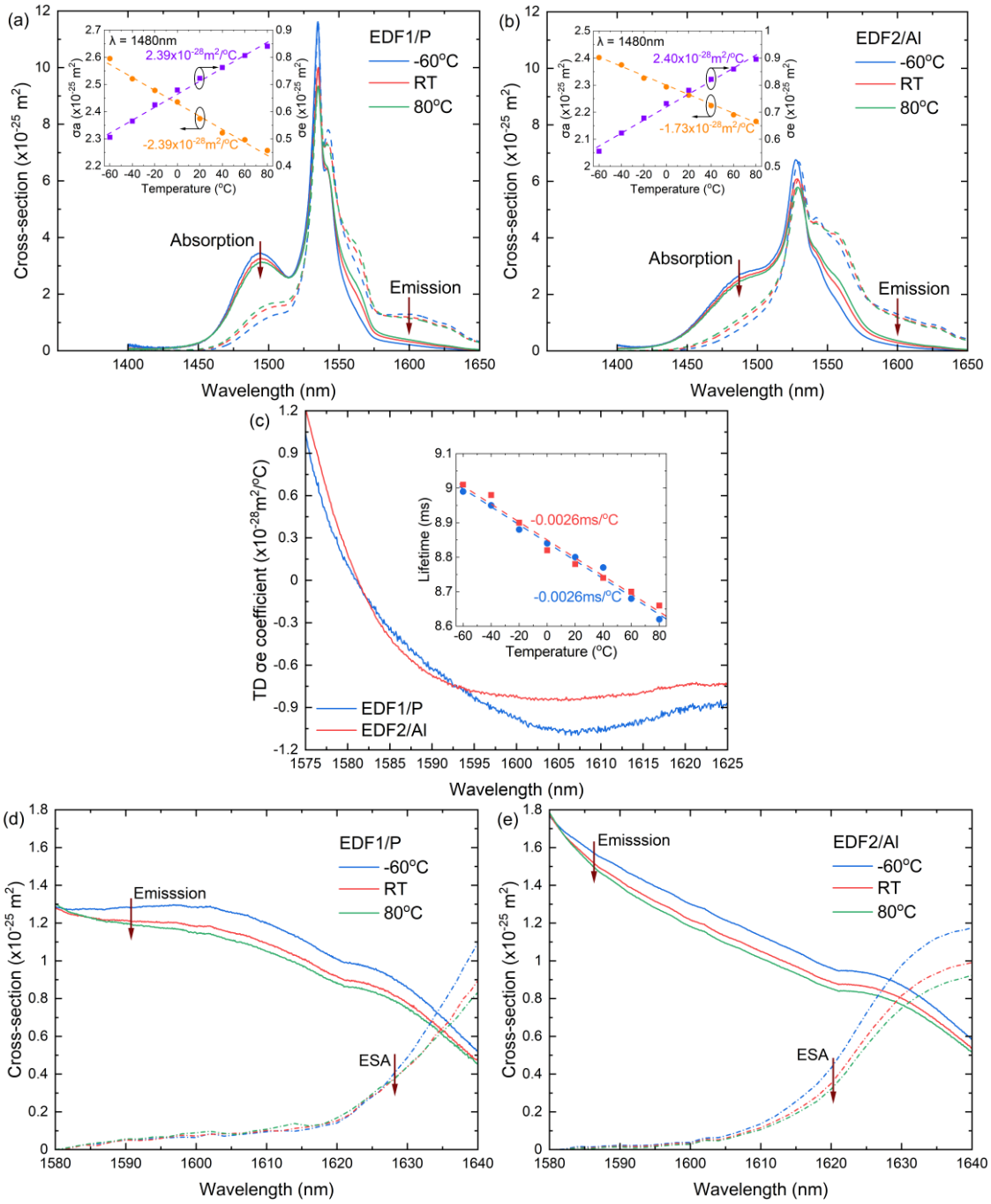

Fig. 1. Absorption and emission cross-sections at -60°C, RT, 80°C for (a) EDF1/P and (b) EDF2/Al (the insets show the TDσ at 1480nm); (c) TDσ_e coefficients in the signal band (the inset shows the temperature-dependent lifetime) for EDF1/P and EDF2/Al; Emission and ESA cross-sections at -60°C, RT, 80°C for (d) EDF1/P and (e) EDF2/Al. (The arrow direction indicates the direction of temperature increases.)

EDFs was very similar, which linearly decreases with the temperature, as shown in the inset of Fig. 1 (c).

$$\sigma_e(\lambda) = \frac{1}{8\pi n^2 c\tau} \frac{\lambda^5 F(\lambda)}{\int \lambda F(\lambda) d\lambda} \tag{5}$$

$$\sigma_a(\lambda) = \sigma_e(\lambda) \exp\left[\frac{hc/\lambda - \varepsilon}{k_B T}\right] \tag{6}$$

As temperature decreased, σ_a at the pump wavelength, σ_e at signal wavelengths (>1580nm) and the lifetime increased. Accordingly, it was predicted to have a higher gain at a lower temperature. At the longer wavelength side of the L-band, signal ESA dominates thus limiting the amplifier performance [16]. Temperature-dependent σ_{esa} were obtained from measured pumped and unpumped transmission spectra and numerical calculations [17], as shown in Fig. 1 (d) and (e). At RT, the cross points of σ_e and σ_{esa} were 1634.9nm and 1629.8nm for EDF1/P and EDF2/Al, respectively. The 5.1nm redshift in the cross point of σ_e and σ_{esa} and the 5.7nm redshift of the Er absorption peak predicted that EDF1/P would have a potential

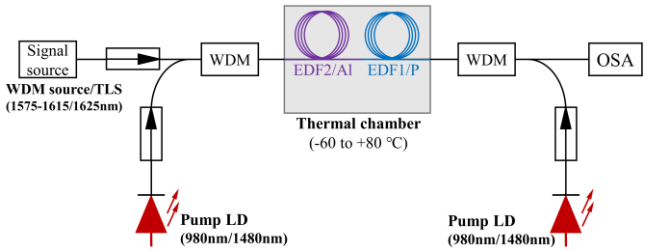

Fig. 2. Schematic of the experimental setup for the L-band EDFA.

shift in the gain peak to longer wavelengths. The cross point of σ_e and σ_{esa} redshift at a higher temperature and EDF1/P has a less cross point shift with temperature.

III. Experimental Setup

The schematic of the EDFA experimental setup is shown in Fig. 2. Laser diodes (LDs) at the wavelengths of 1480nm or 980nm were used to provide FW/BW pumps. Isolators (ISOs) were used to prevent back reflections. Wavelength division multiplexers (WDMs) were used to combine and separate the pump and signal. One WDM source was used to provide the 24-channel input signal from 1575 to 1615nm, with an average of -25dBm power in each channel. In addition, we used a tunable laser source (TLS) to provide a single-channel signal with the power of -25dBm, which can cover the longer wavelength up to 1625nm. An optical spectrum analyzer (OSA, YOKOGAWA AQ6370) with a resolution of 0.2nm was used to measure the input and output spectra. To characterize the temperature performance, a thermal chamber was used to control the environmental temperature of the EDF from -60 to 80°C.

IV. Experimental Results and Discussion

We first measured the multi-channel signal gain and NF at RT pumped at 1480nm and 980nm for a single 30m of EDF1/P and 20m of EDF2/Al, respectively, as shown in Fig. 3 (a). The FW/BW pump powers were 350/350mW for EDF1/P and 400/400mW for EDF2/Al. The gain for EDF1/P was found to be 16.9±1.8dB and 19.4±1.4dB at RT when pumped at 1480nm and 980nm, respectively. The gain for EDF2/Al was found to be 21.5±6.3dB and 20.7±4.9dB at RT when pumped at 1480nm and 980nm, respectively. A better gain flatness was achieved for the 980nm pump wavelength, with no significant change in NF. We measured temperature-dependent gain and NF for the two EDFs over the range of -60 to 80ºC. Fig. 3 (b) shows the TDG coefficient, defined as the slope of the linear regression fit between the gain and the temperature. For EDF1/P, the TDG coefficient varied from -0.018 to -0.065dB/ºC (pumped at 1480nm) and from -0.013 to -0.050 dB/ºC (pumped at 980nm). For EDF2/Al the TDG coefficient varied from -0.002 to -0.048 (pumped at 1480nm) and from 0.017 to -0.028 (pumped at 980nm). Experimental results demonstrate that L-band EDFA is more temperature-sensitive when pumped at 1480nm than pumped at 980nm, which is consistent with the prediction of temperature-dependent cross-sections. At both pump wavelengths, EDF1/P achieved a higher gain at longer wavelengths but was more temperature-dependent.

Next, we measured temperature-dependent gain and NF for

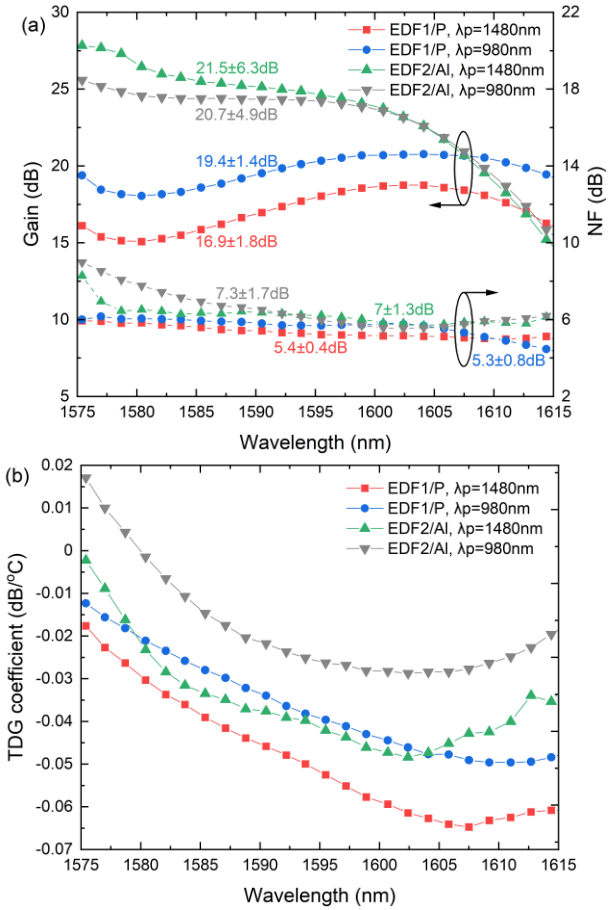

Fig. 3. (a) Multi-channel gain and NF spectra at RT and (b) TDG coefficient spectra for 30m of EDF1/P and 20m of EDF2/Al equally pumped at 1480nm and 980nm, respectively.

the two EDFs pumped at 980nm with FW/BW pump powers of 620/145mW, as shown in Fig. 4 (a) and (b). With a similar gain performance, unequal FW/BW pumping configuration provided a less NF than equal FW/BW pumping configuration. Fig. 4 (c) shows the TDG coefficients for two EDFs when using unequal (solid line) and equal (dashed line) FW/BW pumps, respectively. Unequal pumping was less temperature-sensitive. In the 40nm bandwidth from 1575 to 1615nm, the TDG coefficient under unequal pumps varied from -0.006 to -0.044 dB/ºC for the EDF1/P and from 0.011 to -0.023 dB/ºC for the EDF2/Al. The gain of the EDF2/Al dropped significantly beyond 1605nm, while the EDF1/P maintained a relatively high gain and provided a 3.6dB gain improvement at RT and a 5.9dB gain improvement at -60ºC at 1615nm over the EDF2/Al, demonstrating that P is an effective co-dopant to improve the L-band gain bandwidth. EDF1/P also maintained good gain flatness. However, in both cases of unequal and equal pumps, EDF1/P was more temperature-sensitive than EDF2/Al.

Ideally, a combination of EDF1/P and EDF2/Al is desirable to overcome the longer wavelength limit of L-band gain in the EDF2/Al and compensate for the temperature sensitivity of EDF1/P. The hybrid configuration was optimized using 7.5m of EDF2/Al and 15m of EDF1/P. The hybrid EDF unequally pumped at 980nm achieved 20.9±3.9dB gain and 3.7±0.6dB NF at RT, and 22.2±2.9dB gain and 3.3±0.3dB NF at -60ºC, as shown in Fig. 4 (a) and (b). The gain improvement at 1615nm

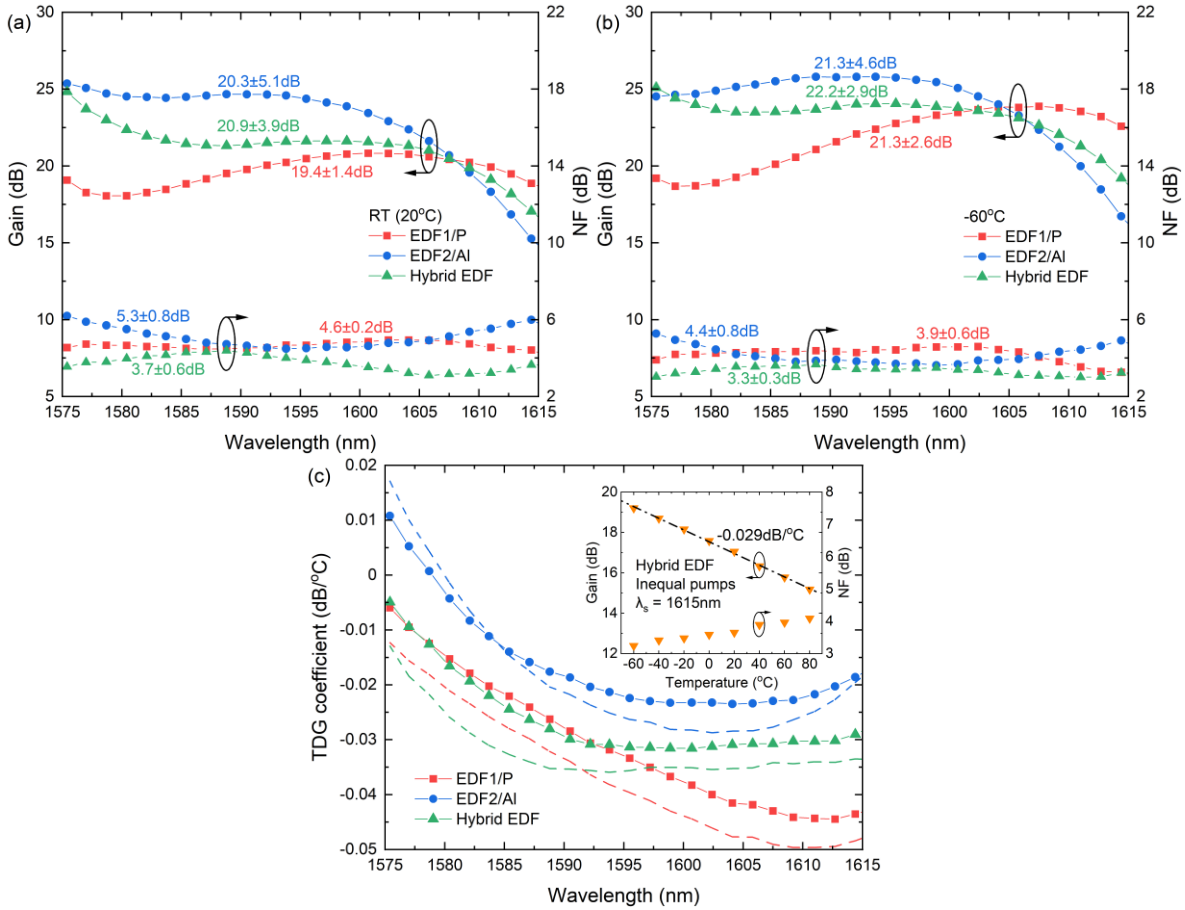

Fig. 4. (a) Multi-channel gain and NF spectra at RT and (b) -60°C for 30m of EDF1/P, 20m of EDF2/Al, and hybrid EDF comprising 7.5m of EDF2/Al and 15m of EDF1/P pumped at 980nm with 620/145mW FW/BW pump powers; (c) TDG coefficient spectra for the 3 EDFs pumped at 980nm using unequal (solid line) and equal (dashed line) FW/BW pumps (the inset indicates the TDG at 1615nm for the hybrid EDF).

was 1.8dB at RT and 2.5dB at -60°C over EDF2/Al, with a less NF than the single EDF configurations. In the 40nm bandwidth from 1575 to 1615nm, the TDG coefficient of hybrid EDF slightly varied from -0.005 to -0.032dB/°C and from -0.013 to -0.036dB/°C when using unequal and equal pumps, respectively, as shown in Fig. 4 (c). From 1585 to 1615nm, the TDG coefficient had a negligible variation of 0.007dB/°C and 0.003dB/°C when using unequal and equal pumps, respectively. Accordingly, hybrid EDF maintained a constant overall gain increase as the temperature decreased in this 30nm bandwidth, indicating a temperature-insensitive gain flatness.

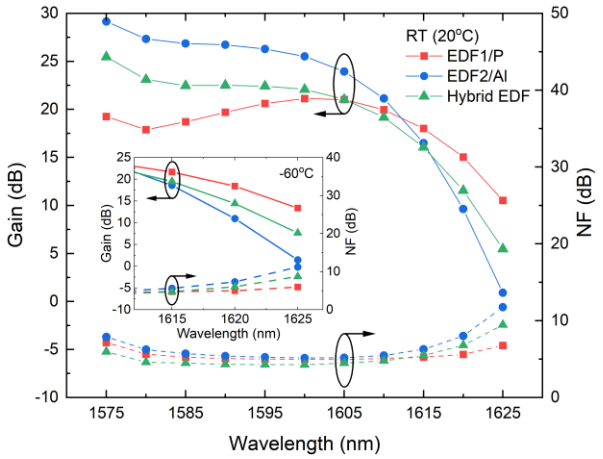

Fig. 5. Single-channel gain and NF spectra at RT for 30m of EDF1/P, 20m of EDF2/Al, and hybrid EDF comprising 7.5m of EDF2/Al and 15m of EDF1/P pumped at 980nm with 620/145mW FW/BW pump powers (the inset indicates the gain and NF at -60°C).

In addition, we used TLS with the input power of -25dBm to measure single-channel signal gain and NF, which can cover a longer operating wavelength up to 1625nm. At 1625nm, EDF1/P maintained >10dB gain with a 9.6dB and 12dB gain increment than EDF2/Al at RT and -60°C, respectively. Hybrid EDF achieved 5.5dB and 7.6dB gain at 1625nm at RT and -60°C, respectively. Average NF at RT was 6.6dB, 5.5dB, and 5.4dB for EDF2/Al, EDF1/P, and hybrid EDF, respectively. Average NF at -60°C was 6.1dB, 4.9dB, and 4.6dB for EDF2/Al, EDF1/P, and hybrid EDF, respectively. This study indicates that phosphorus is beneficial in extending the longer wavelength limit of L-band gain in the silica EDFs.

V. Conclusion

In this paper, we demonstrate that our in-house fabricated EDF1/P is advantageous in extending the gain bandwidth of the operational L-band to a longer wavelength compared to a conventional EDF2/Al. At 1625nm, EDF1/P maintained >10dB gain with a 9.6dB and 12dB gain increment than EDF2/Al at

RT and -60ºC, respectively. However, EDF1/P exhibited a more temperature-sensitive gain. An optimized hybrid configuration consisting of EDF2/Al and EDF1/P was proposed to optimize the temperature-dependent amplifier performance in the L-band. In the hybrid configuration, the temperature-dependent gain sat between EDF1/P and EDF2/Al, and the NF was lower than single EDF configurations. Also, we achieved a flattened TDG coefficient from 1585 to 1615nm, indicating a temperature-insensitive gain flatness in the 30nm bandwidth. Different pumping configurations were studied to evaluate the temperature-dependent amplifier performance, including two pump wavelengths of 980nm and 1480nm and equal and unequal FW/BW pump powers. The pump wavelength of 980nm was more beneficial with the better gain flatness, higher gain at the longer wavelength, and less temperature-sensitive gain. With a similar gain performance, unequal FW/BW pumping configuration exhibited less NF and less temperature-sensitive gain. On the other hand, the experimental temperature-dependent amplifier performance matched with the predictions from the temperature-dependent spectroscopic study based on the cross-sections and lifetime measurements. Our experimental data and comparative study on EDF1/P and EDF2/Al could be further used for the temperature-dependent EDFA modeling.

ACKNOWLEDGMENT

The data for this work can be accessed at the University of Southampton Institutional Research Repository doi: https://doi.org/10.5258/SOTON/D2085.

REFERENCES

[1] A. J. G. Ellison, D. E. Goforth, B. N. Samson, *et al.*, "Extending the L-band to 1620 nm using MCS fiber," in *OFC*, San Diego, California, United States, paper TuA2.1, 2001.

[2] A. Mori, T. Sakamoto, K. Kobayashi, *et al.*, "1.58-μm broad-band erbium-doped tellurite fiber amplifier," *IEEE J Lightwave Technol.*, vol. 20, no. 5, pp. 822-827, 2002.

[3] M. Kakui, and S. Ishikawa, "Long-wavelength-band optical amplifiers employing silica-based erbium doped fibers designed for wavelength division multiplexing systems and networks," *IEICE Trans. Electron.*, vol. 83, no. 6, pp. 799-815, 2000.

[4] S. Tanaka, K. Imai, T. Yazaki, *et al.*, "Ultra-wideband L-band EDFA using phosphorus co-doped silica-fiber," in *OFC*, San Diego, California, United States, paper ThJ3, 2002.

[5] C. Berkdemir, and S. Özsoy, "On the temperature-dependent gain and noise figure analysis of C-band high-concentration EDFAs with the effect of cooperative upconversion," *IEEE J Lightwave Technol.*, vol. 27, no. 9, pp. 1122-1127, 2009.

[6] N. Kagi, A. Oyobe, and K. Nakamura, "Temperature dependence of the gain in erbium-doped fibers," *IEEE J Lightwave Technol*., vol. 9, no. 2, pp. 261-265, 1991.

[7] J. H. Lee, W. J. Lee, and N. Park, "Comparative study on temperature-dependent multichannel gain and noise figure distortion for 1.48- and 0.98-μm pumped EDFA's," *IEEE Photon. Technol. Lett.*, vol. 10, no. 12, pp. 1721-1723, 1998.

[8] Y. Im, K. Oh, S. H. Chang, *et al.*, "Reduction of temperature-dependent gain in L-band EDFA using antimony-aluminum codoped silica EDF," *IEEE Photon. Technol. Lett.*, vol. 17, no. 9, pp. 1839-1841, 2005.

[9] Y. Im, S. Han, and C. Park, "Temperature-dependent gain variation reduction in C-band erbium-doped fiber amplifier using phosphorus-erbium-doped silica fiber," *IEEE Photon. Technol. Lett.*, vol. 18, no. 20, pp. 2087-2089, 2006.

[10] F. A. Flood, "Comparison of temperature dependence in C-band and L-band EDFAs," *IEEE J Lightwave Technol.*, vol. 19, no. 4, pp. 527-535, 2001.

[11] C. Giles, and E. Desurvire, "Modeling erbium-doped fiber amplifiers," *IEEE J Lightwave Technol*., vol. 9, no. 2, pp. 271-283, 1991.

[12] A. H. El-Astal, A. M. Husein, and M. S. Hamada, "The temperature dependency of EDFAs in the 1480 nm pumping configuration," *Opt. Commun*., vol. 278, pp. 71-76, 2007.

[13] C. Berkdemir, and S. Özsoy, "An investigation on the temperature dependence of the relative population inversion and the gain in EDFAs by the modified rate equations," *Opt. Commun*., vol. 254, pp. 248-255, 2005.

[14] J. A. Bebawi, I. Kandas, M. A. El-Osairy, *et al.*, "A comprehensive study on EDFA characteristics: temperature impact," *Appl. Sci.*, vol. 8, no. 9, pp. 1640, 2018.

[15] W. J. Miniscalco, and R. S. Quimby, "General procedure for the analysis of Er^{3+} cross sections," *Opt. Lett.*, vol. 16, no. 4, pp. 258-260, 1991.

[16] A. D. Guzman-Chavez, Y. O. Barmenkov, and A. V. Kir'yanov, "Spectral dependence of the excited-state absorption of erbium in silica fiber within the 1.48–1.59μm range," *Appl. Phys. Lett.*, vol. 92, no. 19, pp. 191111, 2008.

[17] J. E. Román, M. Hempstead, C. Ye, *et al.*, "1.7 μm excited state absorption measurement in erbium-doped glasses," *Appl. Phys. Lett.*, vol. 67, no. 4, pp. 470-472, 1995.